Applied Physics A (2019) 125:406
https://doi.org/10.1007/s00339-019-2699-1

Applied Physics A
Materials Science & Processing

Toward deposition of organic solid with controlled morphology on selected surfaces

Kostyantyn Grytsenko[1] · Peter Lytvyn[1] · Yurii Slominskii[2]

Received: 2 March 2019 / Accepted: 6 May 2019 / Published online: 15 May 2019

Abstract
Multilayer organic and inorganic systems of thin solid films are widely used in novel optoelectronic devices. The required properties of the system depend on the morphology of the films and transition zone at interfaces. We studied the formation of deposits of fluorinated azo-dyes, polymethine, merocyanine and sulfur-terminated organic compounds (STOC) by evaporation and condensation in vacuum. The films were deposited on glass, silicon (Si), gold (Au) and polytetrafluoroethylene (PTFE) substrates. The influence of dye chemical structure and substrate on deposit morphology was studied using atomic force microscopy (AFM). Depending on the ratio between thermodynamic and kinetic processes, islands, crystalline aggregates or nano-structures were obtained. A difference in the morphology of the same dye solid, but deposited on various substrates was detected. Changes in the dye end or side groups caused variation in the morphology of the dye solid film. STOC formed a smooth film on the Au surface, while on the glass and PTFE it formed various islands. Thin films of the dyes in PTFE matrix exhibited unique stability to action of external factors. A new type of evaporable dyes with unsaturated reactive bond at the end was synthesized. Using new evaporation–activation–polymerization methods, the films with enhanced hardness and thermal stability were prepared from new dyes. Several dyes formed nano-micro-wires during the self-assembly process, in some cases between two neighboring Au strips. Adjusting the structure of the molecule by changing the end groups allows purposeful control of the deposit morphology on the selected surface.

1 Introduction

Organic functional compounds (dyes) have been studied for their use in organic light emitting diodes and organic field effect transistors, integrated optic and photonic devices, solar energy converters, etc., since the end of the 20th century. The desired optical properties depend on the chemical structure of the chromophore that is attained during its synthesis. The research was started from the deposition of dye thin films in vacuum [1–3], testing evaporability of the compounds. The knowledge obtained was applied to the explanation of growth processes [4–7]. The backgrounds of formation of the organic solid are necessary for production of the thin films with predetermined properties. The dye molecule has a complex shape and complex three-dimensional distribution of electron density. This peculiarity leads to the formation of different dimers and higher aggregates in the organic solid. Different aggregation states have a low energy of transformation between them, so deposition conditions play an important role in formation of morphology of the solid film. The researchers used for modeling of deposit formation well known "model"—symmetric compounds like 3,4,9,10-perylenetetracarboxylic diimide, [5–9] or the rod-like hexaphenyl [10]. Based on physical forces between molecules and known modes of organic deposit formation (layer-by-layer: Frank-van der Merwe, layer plus island: Stranski–Krastanov, islands: Volmer–Weber), the dimer and larger unit formations for "model" compounds on "model" substrates (mica, Au, NCl, etc.) were simulated together with experimental investigations. Recently, the growth of deposit from the compounds used in industry (Alq_3, pentacene) in multilayer systems was studied [11]. During solid formation, due to concurrent influence of the kinetics and thermodynamics, the amorphous or crystalline films, as well as non-continuous units like islands, wool, nanowires can be formed [6–16]. Sometimes the ability of molecules to form organized domains is necessary, while

✉ Kostyantyn Grytsenko
d.grytsenko@gmail.com

[1] V. Lashkaryov Institute of Semiconductor Physics, pr. Nauky 41, Kyiv 03650, Ukraine

[2] Institute of Organic Chemistry, Murmanska str. 5, Kyiv 02660, Ukraine

in other cases when a smooth uniform film is required, this ability should be avoided. Therefore, understanding of how to control the production of a smooth thin film or nanosized islands and nanowires with predetermined optical properties has been recognized as important scientific knowledge. The self-assembly method was designed to produce the organic deposits with required morphology on the surface of the predefined domains. The nanowires are the new functional units prepared by this method [13–17]. But for self-assembly the molecule has to have different sticking probability on the various materials of the chip. The production of the oriented organic films by deposition in vacuum using hydrogen bonding between molecules was reported [18]. But only a few studies were found on the formation of the deposit morphologies of evaporable asymmetric dyes on solid surfaces. Researches on the applications of the control of the organic functional layer morphology in novel devices continue, showing the importance of this scientific direction [19, 20].

The paper reports research on morphology formation for organic solids by varying the structure of molecules and substrate materials. The new dyes and technologies for production of the thin solid films with required morphology have been designed.

2 Experimental details

Fluorinated azomethine compounds (DP16 and DP21) and azo-dyes (DP01, DP03, DP04, DP05, DP06, DP13, DP17) were synthesized at TH Wildau as described in [21, 22]. Azo-dye DP14 contains the azomethine group as well. The formulae of fluorinated azo-dyes and azomethine dyes are presented in Table 1. Merocyanines, STOC and polymerizable dyes were synthesized at the Institute of Organic Chemistry, Kyiv. They were the bases of asymmetric monomethine cyanine derivatives of benzo[c,d]indole and other donor–acceptor compounds. Synthesis and properties of unsymmetrical monomethine merocyanines 2400–2406 from Table 2 have been described in [23]. These dyes can be considered as donor–acceptor compounds where the acceptor is benzo[c,d]indole residue. Their molecules are not planar, but due to π-stacking they can form dimers. The compounds 7476–7497 are the merocyanines. Their synthesis and properties are described in [24, 25]. The molecules contain bulk *tert*-butyl groups reducing the possibility to form dimers of a "sandwich" type in solid.

The structures of conjugated STOC containing thiocarbonyl terminal groups are presented in Table 3. Their structure is donor-(π-system)-acceptor-sulfur. These compounds were prepared on the basis of rhodanine (2-thioxothiazolidin-4-one) as described in [26]. Polarization and the dipole moment values of these compounds are defined by the electron-donor fragments of the molecules. Table 4 shows the compounds that formed nanowires during deposition in vacuum.

Three-dimensional structures of the molecules and dimers were calculated using Gaussian 09 software. The deposits were produced using upgraded UVN-74 vacuum installation. The starting pressure in the chambers was 10^{-3} Pa. The dyes and Au were evaporated from thermally heated crucibles. The optical spectra of the growing film were recorded in situ using StellarNet and Polytec spectrometers. Depositions on

Table 1 Structure of the fluorinated azo- and azomethine dyes

No.	Structure	No.	Structure
DP 01	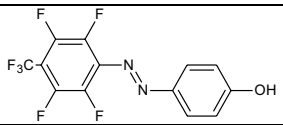	DP 05	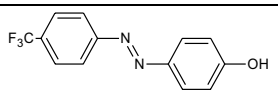
DP 03	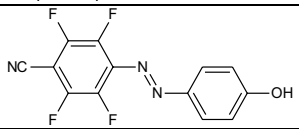	DP 06	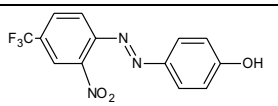
DP 21	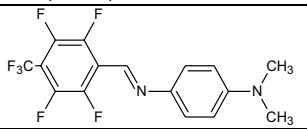	DP 17	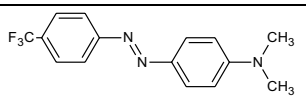
DP 14	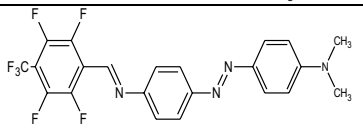	Dp 16	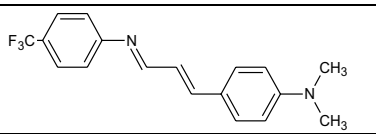
DP 04	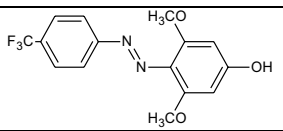	Dp 13	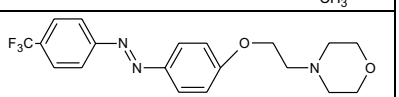

Table 2 Formulae of the merocyanine dyes

No.	Structure	No.	Structure
2400	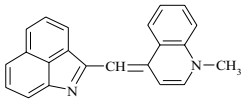	7476	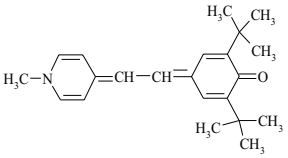
2401	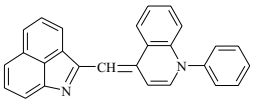	7477	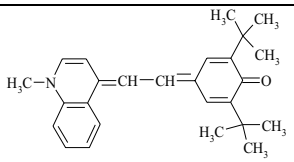
2403	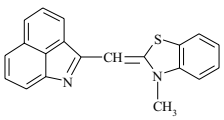	7482	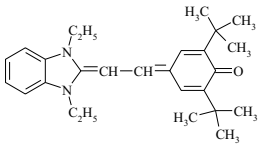
2406	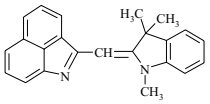	7483	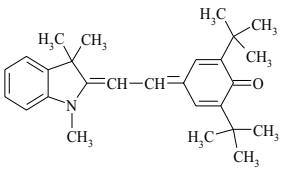
2495	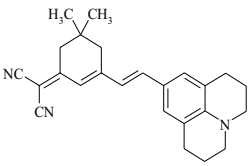	7488	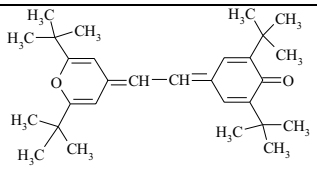
2427	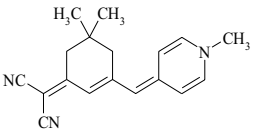	7496	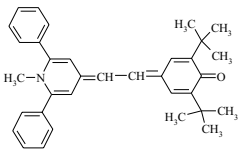
2496	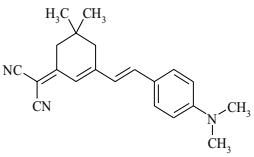	7497	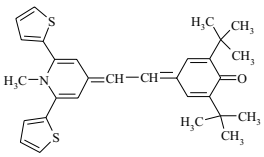

rotating glass disc were finished, when the deposit transmission reached approximately 50% at absorption band maximum. The PTFE films were deposited by decomposition of PTFE pellets and activation of the gaseous products with accelerated electrons. Details of the PTFE deposition can be found elsewhere [27]. The dyes were deposited on Au, glass, Si and PTFE surfaces simultaneously in one run. The morphology of the deposits was studied by the atomic force microscope (AFM) Nanoscope IIIa Dimension 3000™ operated in a tapping mode at ambient conditions. Nanomechanical properties were estimated using the Nanoindentation option of AFM force spectroscopy technique (force–distance curves). Optical spectra during films annealing in air were recorded using a mock-up equipped with a Polytec spectrometer.

Table 3 Structure of the sulfur-terminated organic compounds

No.	Structure	No.	Structure
7626	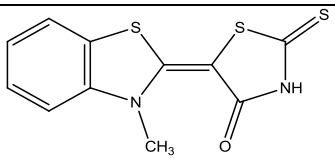	3196	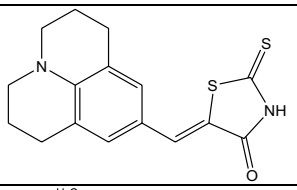
7627	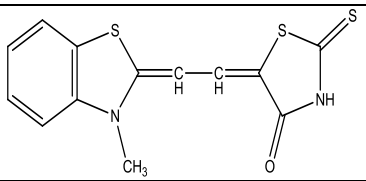	Jb1-11	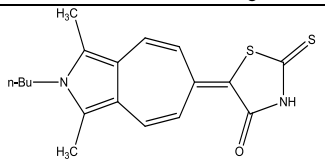
3142	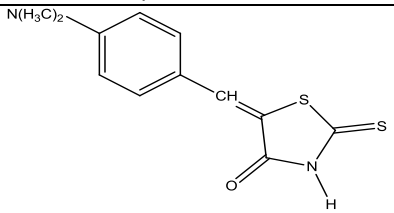	3176	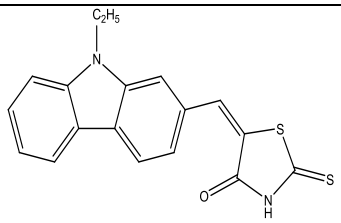
3180	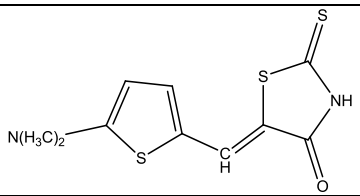	7587	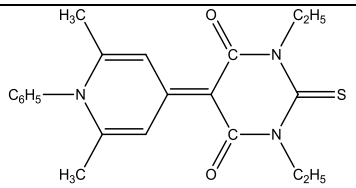
3179	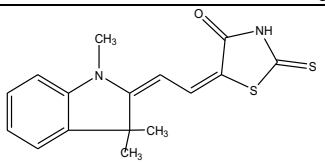	7588	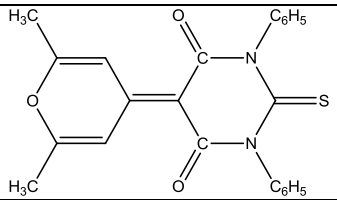

Table 4 Structure of the compounds that produced nanowires

No.	Structure	No.	Structure
3344	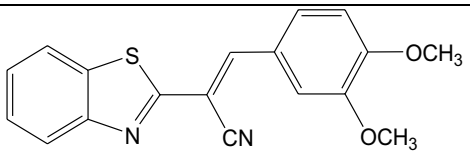	7731	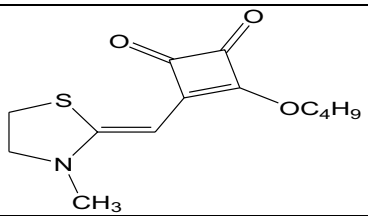
3354	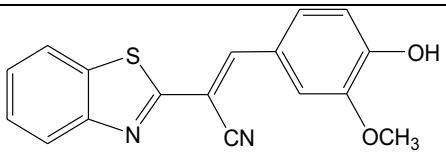	7644	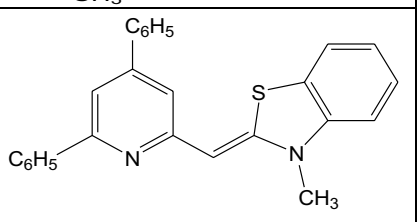

3 Results and discussion

3.1 Morphology of the deposits of fluorinated azo- and azomethine dyes

The deposits of all the dyes were grown on glass with no transformations of optical spectra with film thickness increasing. The absorption bands of the deposits were located around 360–400 nm and represent widened bands of these dyes in solution [28]. Figure 1 shows morphology of the deposits. Depending on the dye chemical structure, variations in the deposits' morphology were found. Relatively small molecules Dp04, Dp05, Dp06 and DP13 formed islands of various shapes. Dp05 formed small round aggregates. Molecules of this type, however, with larger side or end groups formed bigger aggregates. Dp17 formed a non-continuous deposit consisting of connected aggregates with the size of about 2 µm. Dp01 formed a film composed from crystal-like aggregates of several micrometers in length and half micrometer in height. Dp03 formed a structure like Dp01, but aggregates were wire-like shaped up to 3 micrometers long, about 1 µm wide and densely packed. This morphology modification was caused by changing the end group $–CF_3$ in perfluorinated benzene ring in Dp01 molecule with –NC group in Dp03 molecule. Dp21 formed a discontinuous mesh of nanowires together with "bulk" domains. Dp14 formed a "brush" of nanowires up to 500 nm long. This was due to a larger end group in Dp21 molecule and the largest one in Dp014 molecule.

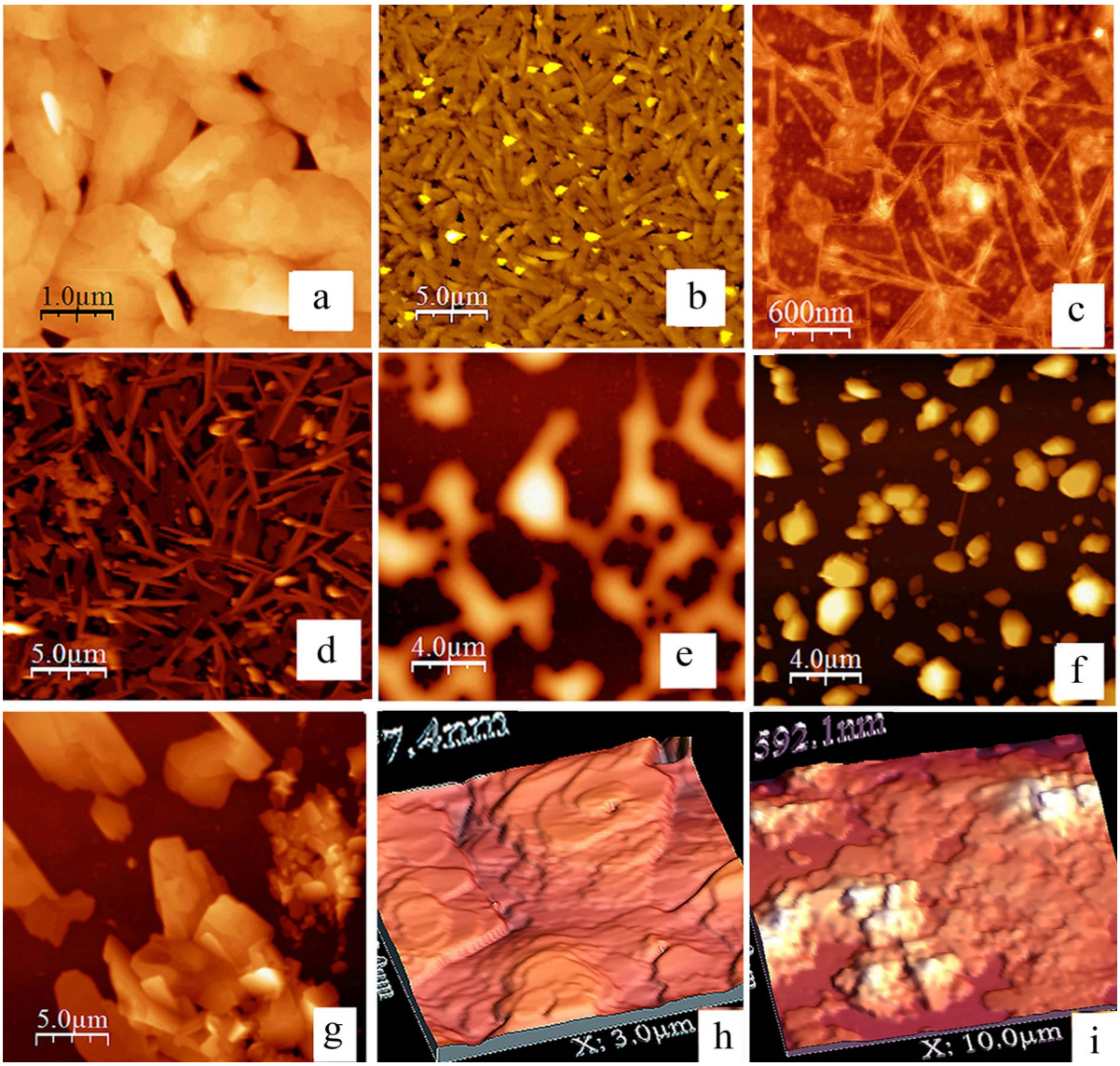

Fig. 1 Morphology of fluorinated azomethine dye deposits: **a** Dp01, **b** Dp03, **c** Dp21, **d** Dp14, **e** Dp04, **f** Dp06, **g** Dp13, **h** Dp16, **i** Dp17

Dp17 formed a continuous deposit but with through holes. The deposit was composed from units with sizes close to 3 μm and aggregated in larger connected units. The change of the azo group in the center of Dp17 molecule with the azomethine group (DP16) led to the formation of a more smooth film with classic terraced aggregates. These experimental data can be used for prediction of the morphology of solid deposits of other molecules of this type.

3.2 Morphology of the deposits of the merocyanine dyes

Figures 2, 3, 4 represent the morphologies of various merocyanine deposits, grown on the glass and the PTFE surfaces. The deposit morphology is dependent on the dye chemical structure, on the substrate material and on the deposition conditions as well [28–30]. The 2400 dye formed aggregates with sizes up to several micrometers on the glass surface. This dye formed the smaller aggregates with size 100–200 nm including elongated ones (up to 500 nm) on the PTFE surface. The dye 2406 formed drops on the PTFE and organized structures like dendrites on the glass. The dye 2401 formed film with aggregate size of about 40 nm on the glass and more rough film on the PTFE. The dye 2495 formed dendrites up to several μm length on the glass, while on the PTFE it formed continuous film with aggregates diameter about 300 nm. The dye 2427 formed film on the glass with aggregates size of about 300 nm, while on the PTFE film had many holes. The dye 2496 formed continuous film with needle-like dendrites (7 μm × 400 nm) on the glass, while on the PTFE it formed discontinuous deposit with organized structures in some domains. Figure 2f is like an image of a surface of polymethine film presented in [31], consisting of herringbone type of molecular arrangement. The similar herringbone structure also can be suggested for the films 2406 and 2496 on glass.

The optical transmission spectra of merocyanine films obtained during their growth showed that many films grew in a stable mode, while several compounds had optical transformation with increasing deposit thickness. The structure rearrangement with film thickness growth was detected for several compounds [12, 17, 28]. The most vivid influence of the substrate material and film thickness on morphology was found for the dye 2403. The 2403 deposit formation on glass began with a continuous film consisting of aggregates with the size of up to 500 nm. This film exhibited a wide absorption band positioned nearby a monomer band (Fig. 3d, red curve). This spectrum corresponds to the amorphous film structure. The thicker film consisted of round units empty inside (diameter 600 nm, height 60 nm). This film exhibited two absorption bands which shifted to long waves (Fig. 3d, green curve). The thickest deposit on glass with the spectrum consisting of two long wavelength bands had large worm-like aggregates (5 micrometers long, 400 nm wide, height 140 nm), composed from joined small units. On the PTFE surface, the more smooth film was formed at an initial stage, but with the increase in film thickness the nanowires were formed on the film. No optical changes during 2403

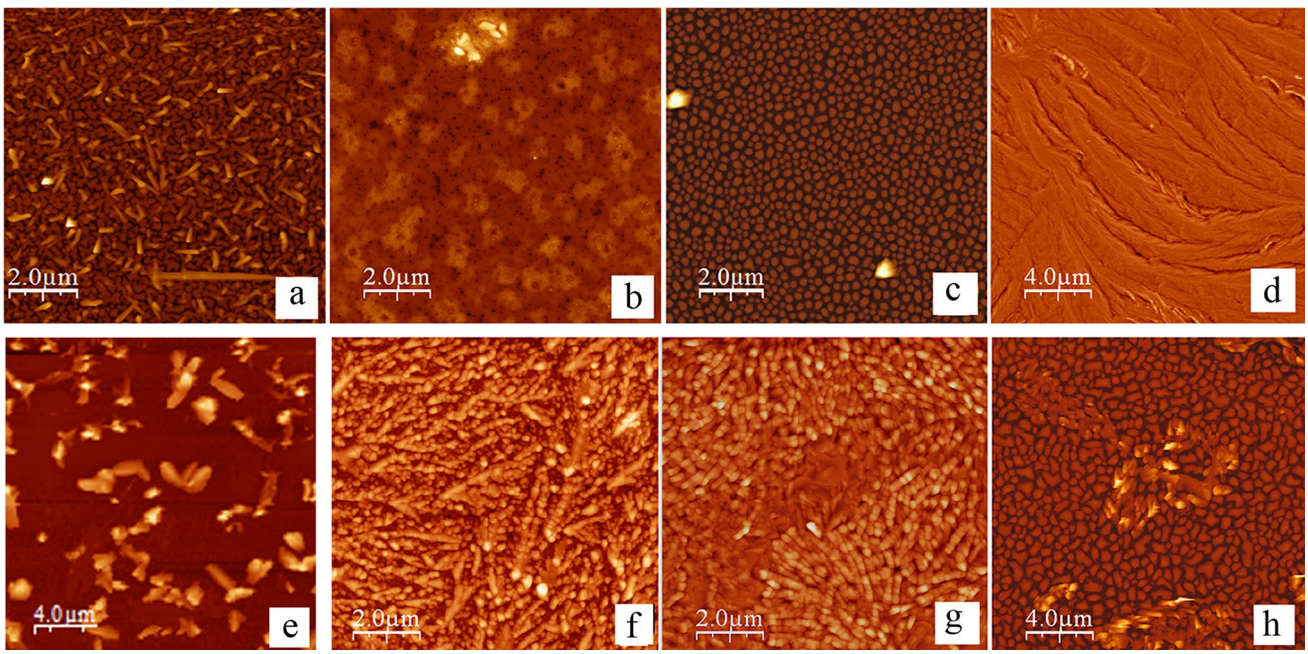

Fig. 2 Morphology of merocyanine deposits: **a** 2400, **b** 2401, **c** 2406 all on the PTFE; **d** 2406, **e** 2400, **f** 2495, **g** 2496 all on the glass; **h** 2496 on PTFE; **b** and **e** reproduced with permission from Grytsenko et al. [28]

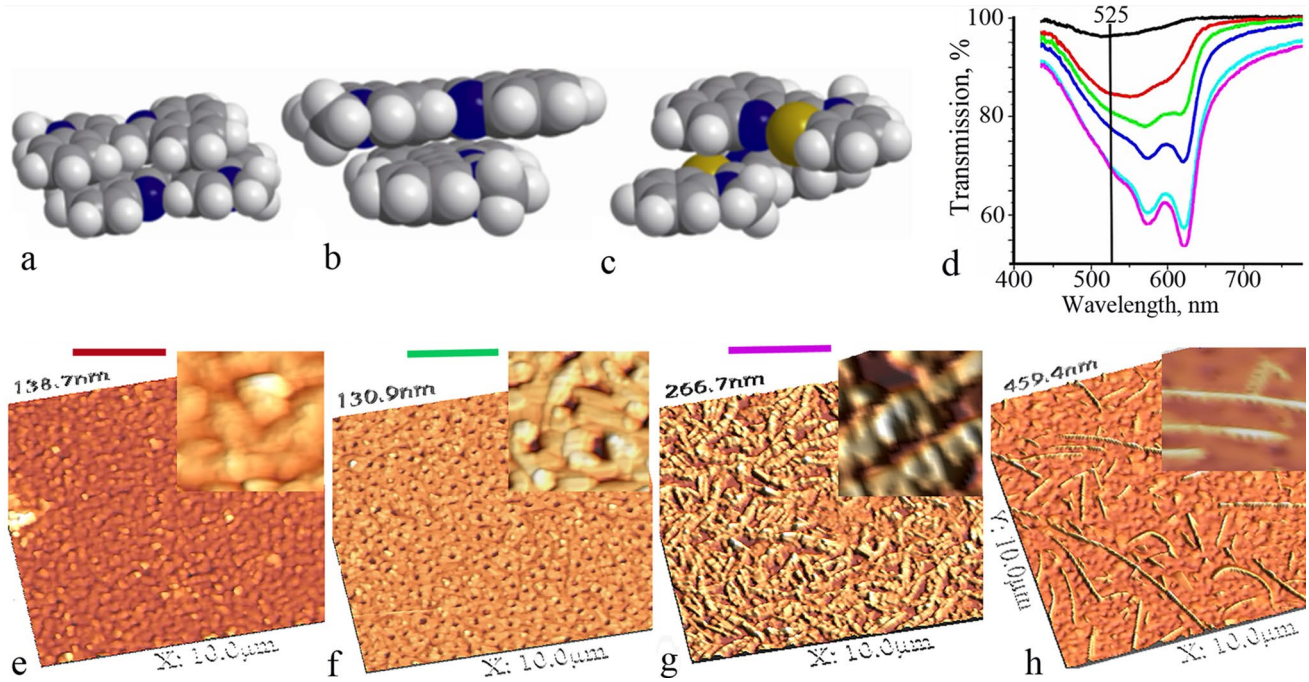

Fig. 3 Morphology of the merocyanine 2403 films. **a**–**c** possible dimers of dyes, **a** parallel dimer, **b** X-type dimer, **c** V-type dimer; **d** optical transmission spectra recorded during deposit growth on glass, vertical line shows monomer absorption; **e** thin dye film, **j** thicker film, **k** the thickest film, all on glass; **h** dye film on PTFE; inserts show magnified images of morphologies. The color lines in the images **e**, **f**, **g** show which spectrum in **d** corresponds to the morphology in the image. **a**–**c** Reproduced with permission from Sieryk et al. [30]. **d** Reproduced with permission from Grytsenko et al. [28]

film growth on PTFE were detected. But no spectrum was taken from a single nanowire.

Transformation of the optical spectrum during deposit growth suggests changes in aggregation and/or molecular orientation relative to the substrate surface. The formation of dimers and higher aggregates of merocyanine compounds was modeled in [32]. Strong inclination of the merocyanine dyes to form dimer-based aggregates was shown. Calculation of the aggregation of merocyanine molecules made in [30] and recently extended in [33], we consider to be suggestive, which require verification by experimental measurements. Various aggregates can be formed in dependence on the molecule structure. Deposit formation of 2400 and 2401 dyes started from dimers. Modelling showed that the molecules in the dimer are parallel to one another (Fig. 3a). The dimers tend to create higher aggregates as stacks. The thin deposit of 2403 dye consisted of molecules in monomeric state, the dimers and aggregates were formed with the film thickness growth. The presence of sulfur atoms led to a decrease in the magnitude of dipole moment of 2403 molecule and changed its direction relative to the chromophore. This dipole momentum is in the plane of the chromophore but at some angle to the main axis, which leads to the formation of another type of dimer. The V-shaped dimers can cause a shift of the absorption band of the film in the long wavelength region and to the formation of two close absorption maxima in the spectrum. In [33] the authors stated that 2403 molecules formed J-aggregates in the film due to a non-planar shape of the molecule, but no reliable explanations except the film optical spectra were presented. Esteban [34] showed that changes in the structure of several merocyanine molecules led to formation of deposits with different morphologies on $Si/SiO_2/AlO_x$ substrates modified with *n*-tetradecylphosphonic acid layer. These dyes displayed an almost planar π-scaffold, where the donor and acceptor units are slightly twisted out of the plane, with torsion angles varying from 3° to 15°. The arrangement of molecules was divided into three types: (1) centrosymmetric dimer with no π-contact to the neighboring molecules, (2) stack of slipped antiparallel dimer units featuring π-overlapping with the neighboring molecules, (3) molecules with equidistance to the upper and lower neighbor in a staircase-like conformation. Near the one stair, the next stair is formed with the oppositely directed dipole moment. This is a herringbone type arrangement. Liess [35] continued the study of structure–property relationships in solid films of new merocyanine dyes. Different morphologies were formed on substrates modified with a layer of *n*-tetradecylphosphonic acid, depending on the chemical structure of the molecules. X-rays and selected area electron diffraction were used to determine molecular packing in the films. The packing of the molecules is governed by long-range dipole–dipole

interaction. This leads mainly to antiparallel packing of the molecules. The three-dimensional shape of the molecule also influences molecular packing. The author pointed out that properly positioned bulky substituents prevent formation of isolated dimers and leads to the formation of a longitudinally slipped dimer stacks. We studied the morphology of solid films of merocyanine dyes of similar types, but with a different chemical structure of molecules. Some features of the merocyanine deposits can be explained by formation of the dimers almost instantly during the molecules condensation. The merocyanine solid can contain dimers both in a disordered state and in ordered stacked domains. The ratio between non-stacked dimers and ordered stacks can be varied with the molecule structure, material of surface and film thickness. The formation of morphology on the macro-scale (as compared to molecule and dimer sizes) is a more complex task to explain. It should include both thermodynamics and kinetics of the deposit growth.

The dye 7476 formed deposit with aggregates with a diameter of about 600 nm on glass. From the dye 7477 to the dye 7483 deposits became more continuous with smaller morphological units. The structural units of the dyes 7496 and 7788 on glass are smaller than the units on PTFE. The dye 7497 film on glass had aggregates about 0.5 µm diameter and 7 nm high, while aggregates on PTFE were 0.2 µm in length, but 20 nm in height. The structure rearrangement with film thickness increase was found for 7497 compound. Two peaks at 625 nm and nearby 700 nm are a feature of a 7497 thin film on both glass and PTFE (Fig. 4a, b). These bands can be explained by the presence of the amorphous phase and J-aggregates in the films. The dye 7497 showed a new short wavelength band of 575 nm on glass with film thickness growth, whereas only monomeric and long wavelength bands were present in the spectra of the films on PTFE. H-aggregates were formed in the 7497 film with its thickness growth on glass (Fig. 4d), but not

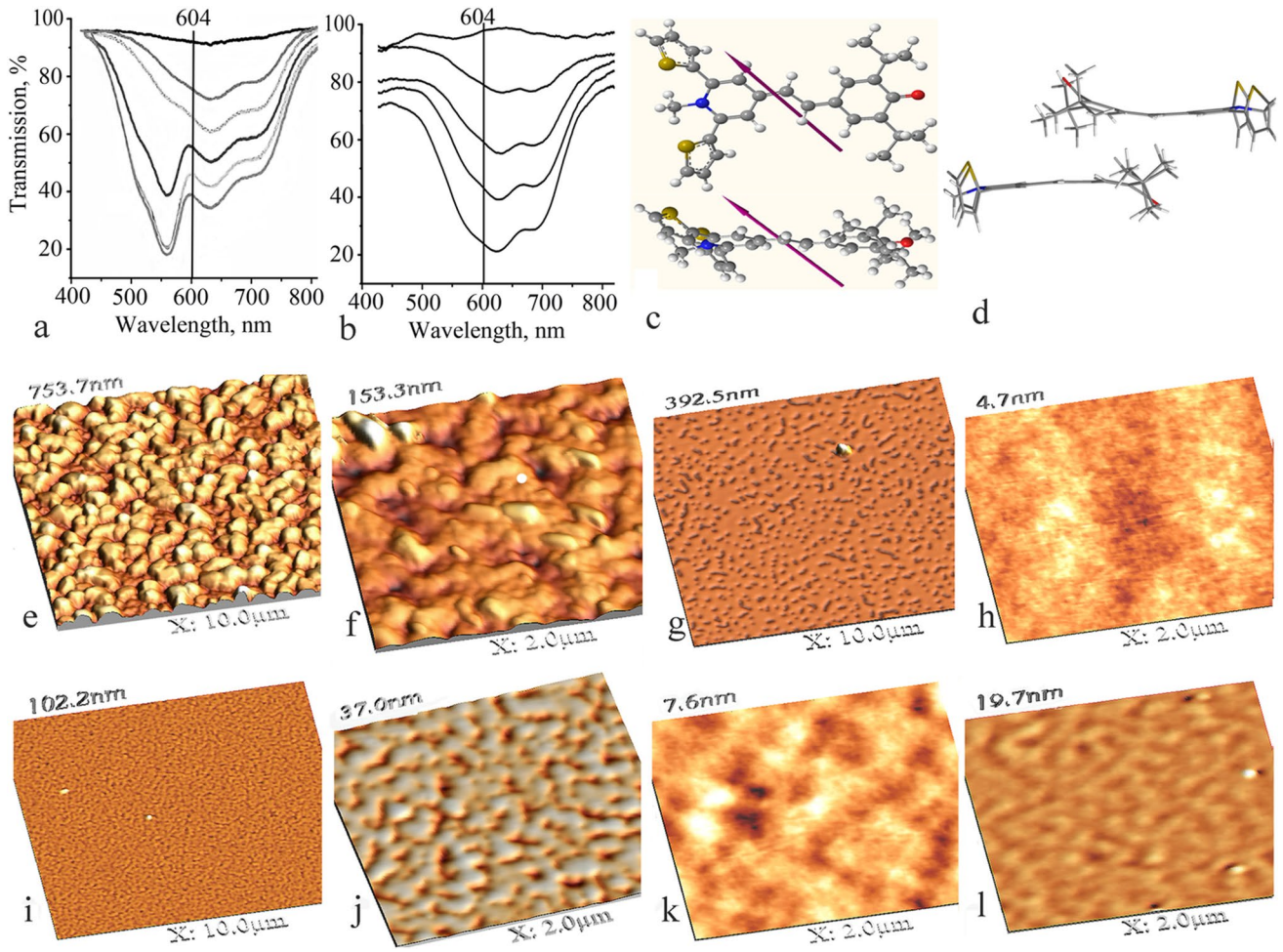

Fig. 4 Optical spectra recorded during merocyanine deposits growth and morphology of the deposits: **a** and **b** optical spectra recorded during 7497 deposit growth on glass and PTFE, respectively, the vertical lines show monomer absorption, **c** structure of the 7497 molecule and **d** dimer; **e**–**h** and **k** morphology of the films 7476, 7477, 7482, 7483 and 7497, all on the glass; **i** (**j** magnified **i**) 7496 and **l** 7497 on the PTFE; **a** and **b** reproduced with permission from Grytsenko et al. [28]

on PTFE. Molecules in dimers on glass formed a shifted structure with the angle 37.5° between the centers of the molecules [29]. Deposits of dyes 7482 and 7496 showed no significant difference in the spectra on both glass and PTFE. The spectra of the deposits of the both dyes have small splitting of the monomer band. The thiophene end group in dye 7497 instead of the benzene end group in dye 7496 leads to formation of the H-aggregates on glass, which starts with a certain film thickness. The changes in dimer formation with end groups variation together with different substrate type and condensation temperature were the explanation of optical and morphological changes in the obtained films [28, 29]. The rearrangement of molecular orientation like that described in [36] for sexithiophene molecules during film formation also should be taken into account.

The substrate surface energy influences the morphology and optical properties of the film. The general rule for continuous film formation is that interaction of dye molecule with the substrate surface should be stronger than molecule–molecule interaction, whilst for islands formation the rule is vice versa. But this is true only for the first surface layer for continuous film mainly with Frank–van der Merwe growth mechanism. The next layers grow without direct influence of the substrate, but it is not equal to zero. The structure of these layers is determined by competition between order ignited by the first layer and equilibrium structure of the dye solid. The ratio between dye–dye and dye–surface interactions defines how far the dye structure will be from the equilibrium one. A good example of the deposit growth mechanism and structure rearrangement was shown for pentacene: when the film thickness exceeds a certain level, the growth shifts from layer-by-layer mechanism to the three-dimensional one and later to ordered structure creation [11]. For perylene, the growth mechanism with molecular rearrangement on different inorganic substrates was shown in [9], starting with the first layer lying flatly on the surface. The deposition rate was shown (modelling for 6P molecules) to be an efficient tool to shift the growth mode from equilibrium to the non-equilibrium one [37]. The vertical standing of a single molecule on substrate is possible, if the interaction energy of molecule's one end with the substrate < evaporation energy < interaction energy of the molecule's second end with the substrate. The smaller molecules with low evaporation temperature tend to form islands and discontinuous deposits [38]. Many small molecules formed aggregates with the sizes close to optical resolution level.

The dye chemical structure, substrate surface energy, condensation temperature, and deposition rate are the factors influencing both thermodynamics and kinetics of the deposit growth. To some extent, the morphology can be controlled by deposition conditions. The variation of the end groups in molecules is an additional method to control morphology of the merocyanine deposits.

3.3 Morphology of the sulfur-terminated dye deposits

Going from knowledge derived from deposit growth studies using "model" compounds (for example, [5–7]) and from our experimental results obtained for asymmetric dyes, the idea to design evaporable dyes exhibiting defined interaction with selected substrate and tuned morphology was issued. The sulfur-terminated dyes are suitable for selective interaction with the gold surface. Au nanoparticles (NPs) functionalized with organic compounds have been studied for photonics and plasmon structures [25, 39], sensors [40–43], photovoltaics [44], medicine [45, 46] and other interdisciplinary areas. But this functionalization was made in a liquid phase. The evaporable STOC were designed and synthesized [26, 47–50]. Morphologies of the STOC deposits on glass, PTFE and Au surfaces are shown in Fig. 5. The difference in morphology on the same substrates and the degree of difference in morphology on a variety of substrates is evident. STOC 7626 and 3179 formed discontinuous deposits with a different size of "bricks" on glass, smaller units on Au and continuous film with smallest aggregates on PTFE. Morphologies of 7627 deposits are similar to those of STOC 7626 on all the substrates. STOC 3180 formed almost no deposit on PTFE, islands on glass and continuous film on Au.

The other STOC formed smooth films on Au surface. On glass surface separated "bricks" and particulated films on PTFE were formed. Morphologies of STOC with the most vivid differences of the morphologies on the various surfaces are presented in Fig. 6. The variations of the morphologies on the different substrates are dependent on the STOC structure. The STOC 3172 formed miserable debris on the all the substrates.

Most of the deposits showed no optical transformations during their growth on all the substrates. The deposit of STOC 7587 showed optical transformations during growth only on glass (Fig. 7). STOC 7587 and 7588 formed continuous film with no aggregates on Au surface at comparatively high-deposition rate of 1 nm/s. The deposit on glass is composed of aggregates. The molecule of 7587 dye is more polar, than the 7588 one, because of the higher electron-donating properties of 1,4-dihydropyridine residue. X-ray photoelectron spectra of 7587 deposit on Au showed the presence of sulfur atoms both bound to Au and unbound ones [26]. Therefore, part of the molecules was chemisorbed on the Au surface.

STOC 3196 formed elongated aggregates like dendrites (10 μm × 1 μm × 250 nm) on the Au surface, but almost no deposit on PTFE and drops with diameter about tens nanometers on glass (Fig. 8). It seems that on PTFE and glass the ratio between condensation and evaporation kinetics of 3196 dye was close to the equilibrium. The dendrites indicate that molecules have high mobility on the Au surface, and

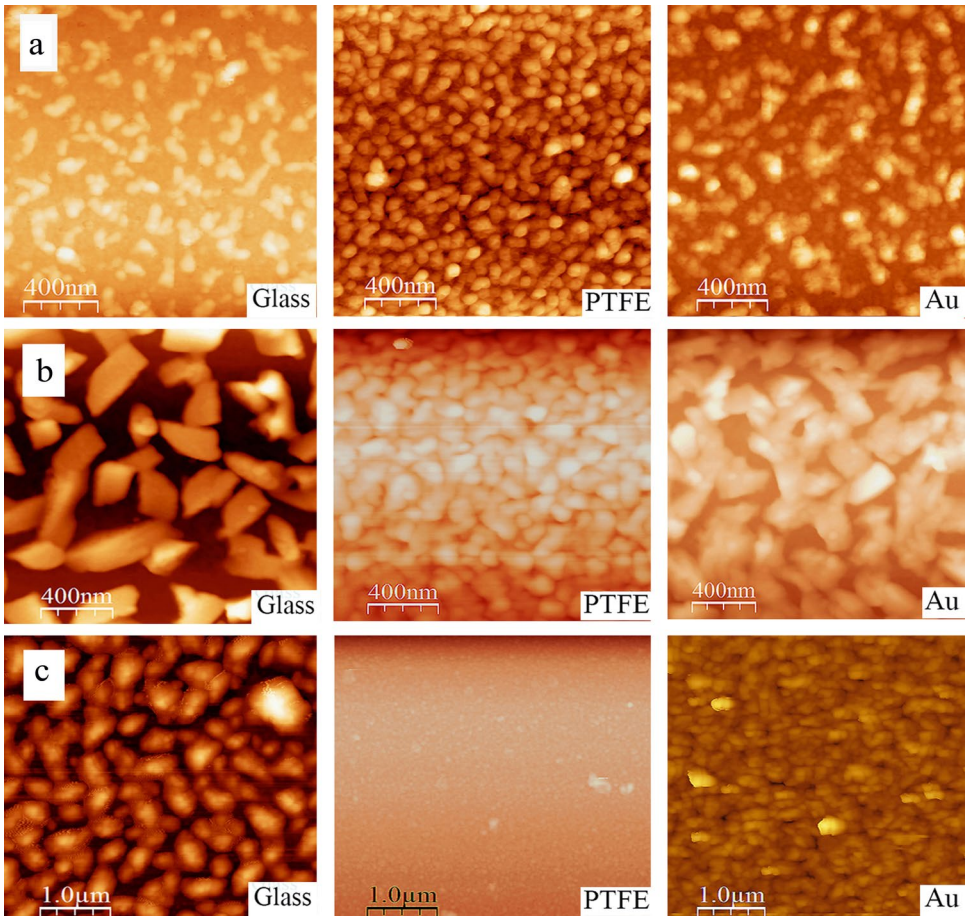

Fig. 5 Morphology of the STOC deposits on different substrates: **a** 7626, **b** 3179, **c** 3180

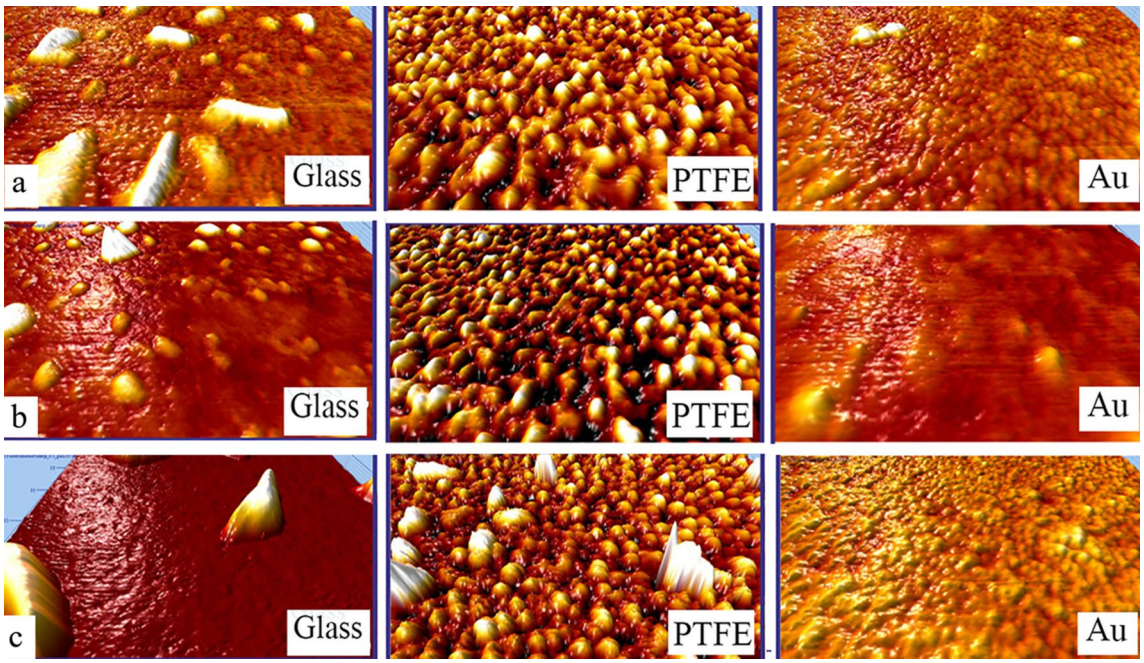

Fig. 6 Surface relief of the STOC deposits: **a** 3142, **b** 7587, **c** 7588. For all images: *x* 2 μm, *y* 2 μm, *z* 20 nm

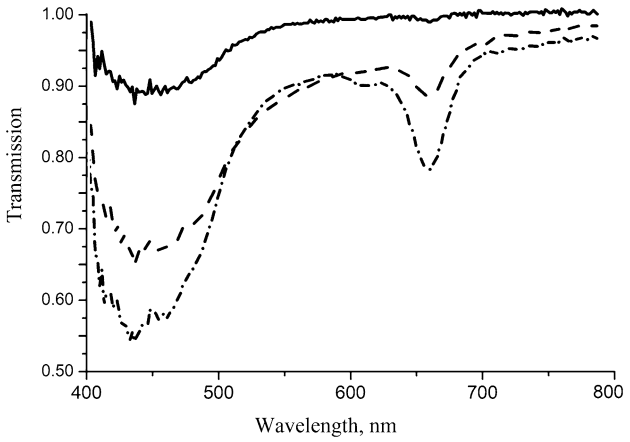

Fig. 7 Optical spectra recorded during 7587 growth on glass with film thickness increase

dye–dye interaction was stronger than interaction of the dye with Au. JB1-11 formed separated islands on glass, continuous rough (heights about 100 nm) film on Au and nanowires (1 μm × 150 nm × 150 nm) on the PTFE surface. The deposit 3196 on glass had a split band with stronger peak nearby 540 nm and the weaker one nearby 485 nm, while on Au only 540 nm sharp peak was present. The deposits of the Jb1-11 had the same spectra on glass, PTFE and Au. Therefore, the same dimers were organized in different macro-morphologies.

3.4 Multicomponent nanocomposite films with PTFE matrix

It is known that dye-filled polymer films have enhanced stability. Therefore, PTFE as the most stable and transparent in thin film form polymer is attractive as a matrix for these dyes. The PTFE films filled with various dyes at different concentrations were produced by co-deposition in vacuum [12, 37]. Optical spectra of the films showed that usually dye molecules were in monomeric state at small and moderate concentrations and did not aggregate up to the dye decomposition temperature. Figure 9 represents comparison of the dye 2403 in polyparaphenylene sulfide matrix and dye-in-PTFE spectra during annealing in air as the vivid example of the influence of PTFE matrix on the film thermal stability. The film of the pure dye was decomposed/evaporated at 110 °C. Films with the PTFE matrix showed unique stability to action of all external factors [51]. The properties of the dye-filled PTFE films cannot be explained as the sum of dye and PTFE properties. Addition of metal nanoclusters to dye + PTFE system enhanced thin film sensitivity to aggressive gasses. The farther design of the

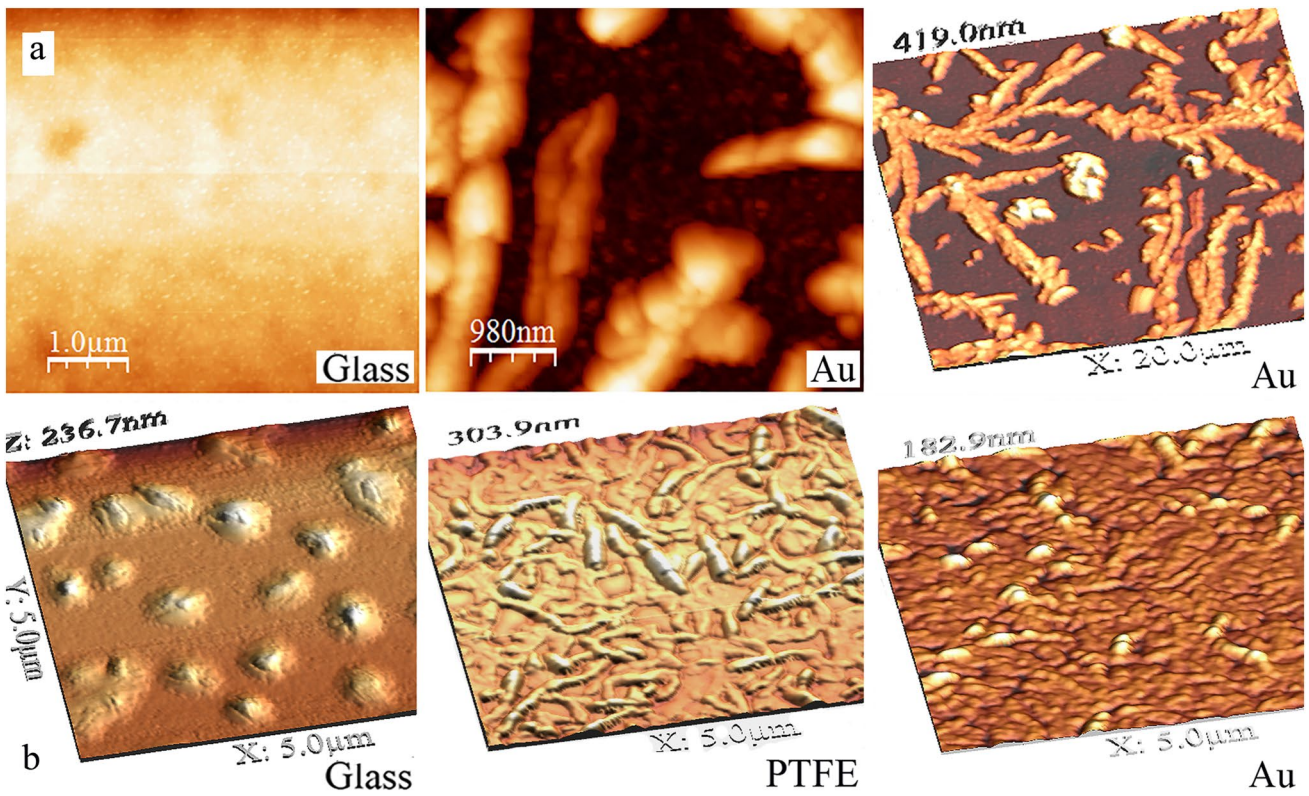

Fig. 8 Morphologies of the STOC deposits: **a** 3196, **b** Jb1-11

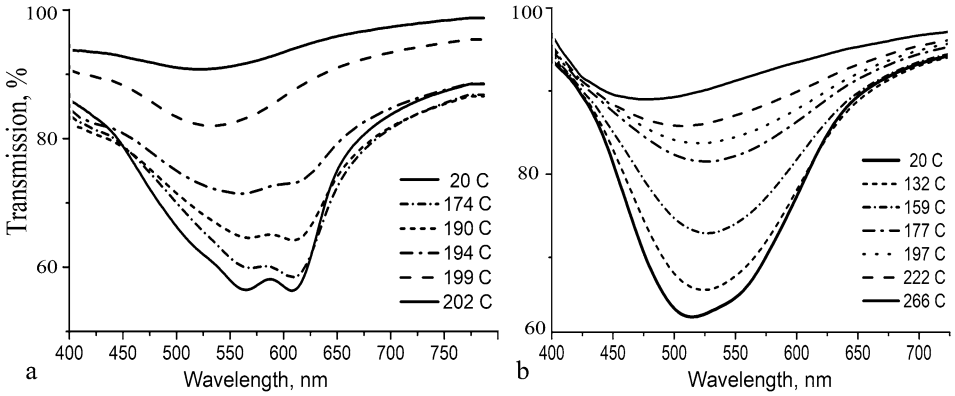

Fig. 9 Optical spectra recorded during annealing in air of the polymer films, filled with dye 2403: **a** dye in polyparaphenylene sulphide matrix, film, **b** dye-in-PTFE

multicomponent thin films will be creation of self-organized nanocomposites [52]. Formation of dye "fur" around Au NPs is possible, as well as formation of dye nanowires, which can connect two Au NPs. Production of this complex film deserves farther studies.

The dye-in-PTFE thin films are promising for optical devices with enhanced stability. The following advance in soft condensed matter technology was attained by design of the new dyes, aimed for their activation in the gas phase (unsaturated end bond selective opening) and consequent polymerization on solid surface [53–55].

3.5 Evaporable dyes with a reactive bond at the end

For other than gold substrates, the compounds able to form chemical bond with surface are required. Creation of the evaporable large reactive organic molecule needed special design. These molecules should have the end group able to react with the substrate surface. Such active molecules can interact with each other producing a polymeric solid. It is known that only a few homopolymers can produce films by macromolecule decomposition and polymerization of active fragments on a substrate surface [27]. Small molecules, mostly the monomers, are "polymerizing" in a glow discharge, producing cross-linked film with the structure not similar to macromolecules in classic polymer. The evaporable molecules containing chromophore with unsaturated bond at the end were designed [53–56]. This end bond was not opened during evaporation, but opened by activation in the gas phase or on the substrate surface. To calculate the molecule was hardly possible due to close values of the energies (E) of the C=C bonds in the molecule. The molecule must satisfy the following rule:

$$\Downarrow \text{ activation action}$$

$$E_{\text{evaporation}} < E_{\text{open unsaturated bond}} < E_{\text{ all other bonds in the molecule}}$$

A lot of various molecules were designed, synthesized and tested. Usually the unsaturated bond was opened during heating and produced polymer in the crucible. Ultimately the satisfying compounds were found out. Started from the first evaporable dyes with a double bond at the end [53, 54], various compounds were obtained [55, 56].

Production of the organic films with optoelectronics properties by plasma "polymerization" from standard molecules is not possible. When plasma treats molecule with the size larger than monomer (chromophore), the molecule is destructed in a random way with loss of its optical properties. Moreover, to ignite the plasma, it is necessary to produce conductive path in a gas, which leads to ionization and decomposition of a part of the molecules. The phthalocyanine [57, 58] and merocyanine [59] compounds were "polymerized" in plasma. The deposits were stable polymers, but their optical absorption was reduced. Part of the molecules was decomposed. Later dye molecules were sublimated and introduced in the glowing discharge in benzene [60]. The authors reported that the part of the dye molecules was damaged. More dyes were "polymerized" in plasma with creation of stable films [61, 62]. From IR-spectra the authors concluded that dye molecules were incorporated in "polymer" film. So, a part of these molecules was decomposed to produce a "polymer" matrix. The classic plasma is not suitable for selective activation of the unsaturated bond in the new compounds. Grytsenko with co-authors found out that decrease of discharge power in monomer gas led to formation of a film with properties close to classic polymer [63, 64].

Several less energetic activation methods were developed for "polymeric" dye films deposition [56]. Dependent on the dye structure, activation conditions and substrate material, the deposits with different morphologies were produced. The films deposited with the best activation conditions were smooth at nano-level (Fig. 10) and showed enhanced nano-hardness (Fig. 11). Morphology and nanomechanical properties of the films were varied by changing activation parameters. Optical spectra of the films deposited with activation contained one monomeric band, instead of the films of the same dyes, but deposited

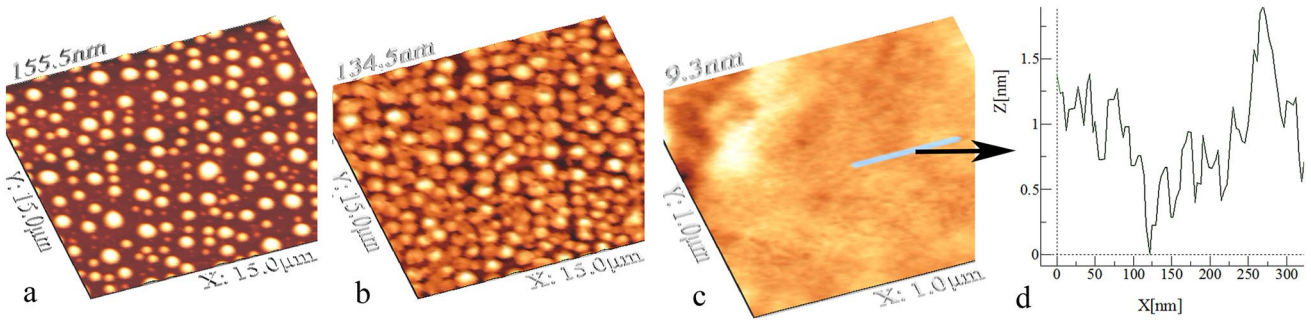

Fig. 10 Morphology of 2566 deposits: **a** deposit on polycarbonate and **b** on glass, both produced by thermal evaporation without activation; **c** film on glass deposited by evaporation with activation, **d** represent the surface relief of the film along the mark

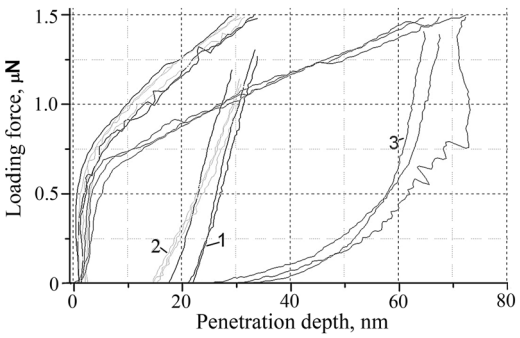

Fig. 11 Load-penetration curves of the films, deposited with different activation methods 1,2,3

without activation. The films deposited with the best activation conditions revealed no transformations of their optical spectra during heating up to the decomposition temperature (Fig. 12). The decomposition temperature for the films deposited with activation was significantly higher than that for the films deposited by thermal evaporation and exceeded the dye evaporation temperature in vacuum.

The film of the dye 2556 deposited without activation was completely decomposed at 90 °C. The films deposited with best activation conditions showed some absorption of pristine chromophore even at 271 °C. The film deposited by simultaneous deposition of the dye and PTFE showed bigger stability than that of pure dye film, but smaller stability, than polymeric dye film. The development only at the first stage: several new types of chromophores were designed for polymerization in vacuum. The technologies for evaporation–activation–polymerization of these dyes were only tested. It is necessary to carry out the research on the activation methods to find the optimal conditions for deposition of the polymeric films with the best properties.

The second set of the new evaporable molecules containing two active functionalities were designed. The organic salts containing unsaturated end group were designed. After their activation upon evaporation, thin films of cationic dye polymers were obtained. The molecules containing core chromophore for photovoltaics, unsaturated group and group for bonding with Au can be synthesized. The developed compounds and deposition

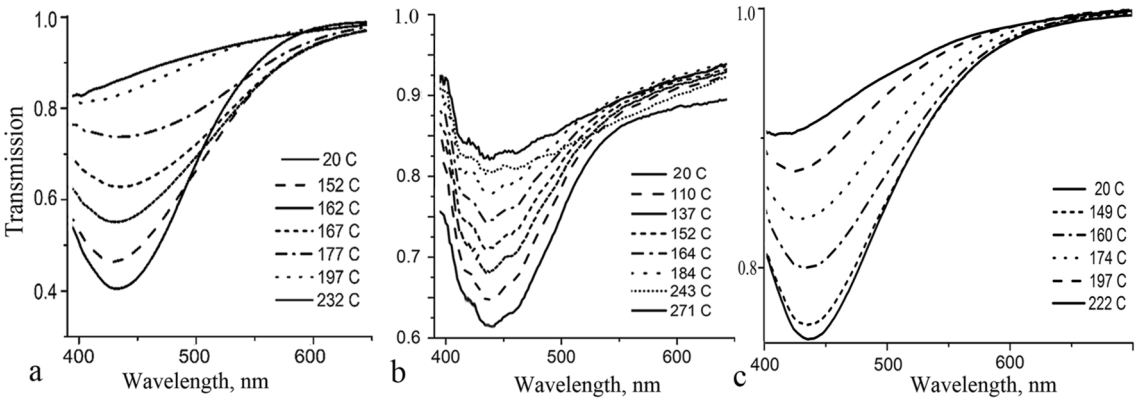

Fig. 12 Optical transmission spectra recorded during heating of the 2566 films in air: **a** and **b** films was deposited by evaporation with different activation conditions, **c** film was deposited by co-deposition together with PTFE

technology discover new direction for creation stable active elements for optoelectronic devices.

3.6 Nanowires in multilayered systems

Several compounds formed nanowires in dependence on the substrate and deposition conditions, in some cases up to several centimeters long (Fig. 13). Mostly the wire-like morphology was formed by molecules containing thiophene in the structure. Though these molecules are different and their formalization by the presence of thiophene seems arbitrary. Nanowires formed from merocyanine containing two sulfur atoms in a 1,3-dithiolane group were shown [34]. Formation of the nanoneedles by thiophene-based "model" molecules on model substrates is well known [65–67]. The growth mechanisms of nanoneedles have been described in these papers.

A few dyes revealed interesting effects during solid formation. The growth of nanoneedles on the PTFE surface with 100 nm wide trench down to Au surface started from PTFE knoll at the trench end, but not on Au surface (Fig. 14a, arrows 1). Some needles crossed the trench above it (Fig. 14a, arrows 2). But if the trench is wider than 20 µm, the nanowires were formed between the gold strips on Si and on PTFE surfaces via self-assembling (Fig. 14b and c). The nanowire (30 µm × 1 µm × 250 nm) is lying on Si surface with both ends attached to two neighbor Au strips. In the researches made before the second end of nanowire was loose [13–16]. The additional efforts were necessary to connect loose end with another surface. Recently, the research concerning self-assembly of nanowires connecting two metal strips has appeared [68]. Three compounds from the tested ones produced almost the same nanowires as those shown in Fig. 14c. The ratio between nanowire length, width and height is different for various compounds. It is the farther research task how to control nanowire geometrical parameters.

The formation of nanowires was caused by interplay of interactions for the three materials of the system (Si, Au, dye). Figure 14d shows the hardness of 2566 nanowire and dye films. The material of the nanowire was softer than the film material, indicating a different organization of the solids. Figure 14e and f presents the surface of nanowires from the 2556 and the 7624 dyes, giving the data concerning the growth mechanisms of the nanowires. The structure of nanowires produced from new compounds is to be studied further. In the terms used by the Winkler [69], the dye 7624 formed "wetting" layer on the Si surface and the nanowire on this layer. The term "wetting" generalizes the final result of the both thermodynamic and kinetic factors actions. We would prefer to describe the formation of a solid substance from the viewpoint of the substrate-dye interactions, which we used since explanation of the merocyanine solid formation. Prolongation of already formed structural units (nanowire formation) is possible, if dye–dye interaction and diffusion rates are not low. The necessity of the high diffusion rate and dye–dye interaction narrows the domain of the suitable thermodynamic and kinetic parameters. Modification of the core chromophore with different end groups leads to variations in the domain of the parameters suitable for nanowire growth.

4 Conclusions

The experimental studies of the morphology of organic solid films produced using known compounds gave impetus to the design of new compounds aimed at the deposition of

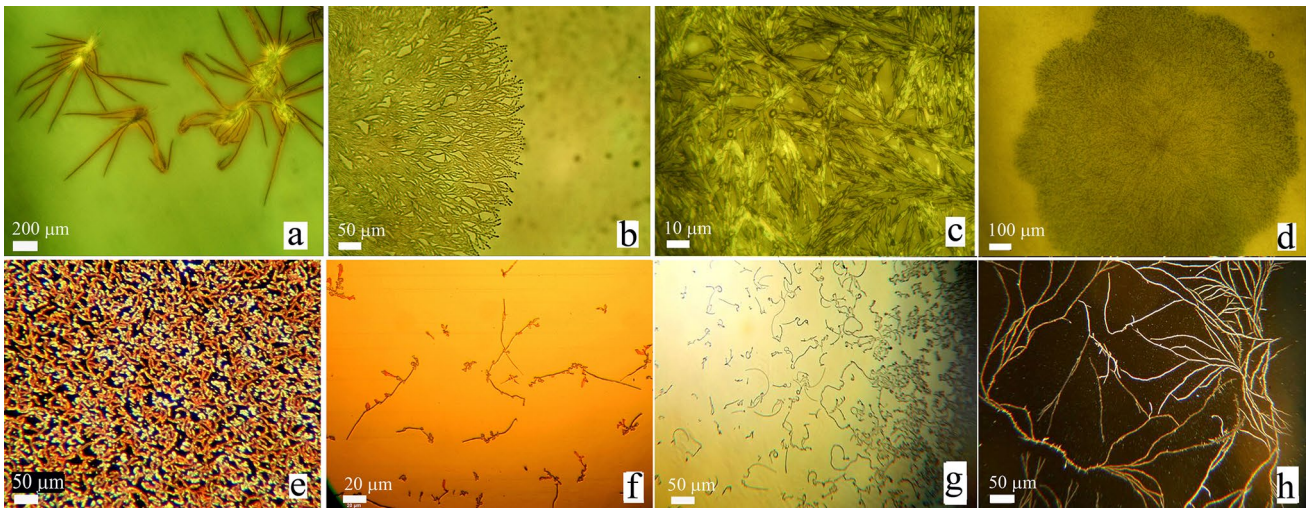

Fig. 13 Optical images of the deposits. **a** 3354, **b** 3344, **c** 7731, **d** 7644, all on glass; **e** 3196 and **f** 7587 on gold; **g** 2566 on glass; **h** 7604 on Si

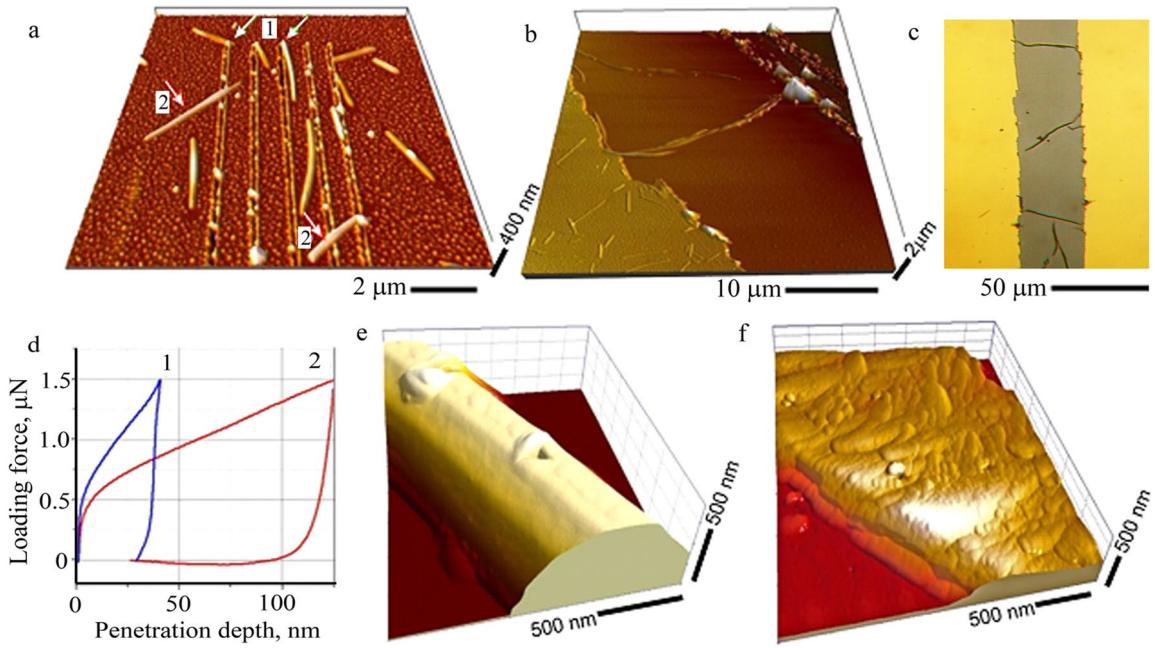

Fig. 14 7624 and 2566 dye deposits in multilayer microstructures: **a** 7624 on narrow trench on PTFE/Au/Si chip, **b** 7624 nanowire on Si between two sides (Au strips) of wide cut, **c** the optical image of the 7624 nanowires, **d** nanoindentation curves of the dye 2566 film 1 and the nanowire 2, **e** the 2566 nanowire (pit from indent on top), **f** morphology of the 7624 nanowire

solid films with a predefined morphology. Optical properties of the organic solid can be constructed at the stage of the molecule synthesis, but deposition conditions also play an important role affecting optical properties through controlled aggregation and orientation of the molecules in the film. Using the core chromophore, but with various end groups, it is possible to control the morphology of the deposits, taking into account the substrate material, thus making it possible the self-assembly of the nanosized organized units or vice versa, to form a uniform film. The sulfur-terminated dyes are the one kind of organic compounds that formed deposits with different morphologies on gold and other substrates. The new evaporable compounds with a reactive group at the end and activation methods for selectively opening of this group led to the production of the smooth and highly stable films. Several compounds of different types formed nanowires. Self-assembled organic nanowires were obtained on the silicon surface between two gold strips. The nanowires made from functional dyes can be used for the production of nanosized optoelectronic devices. The nanowires produced from dyes with a reactive end group can be the building blocks for the creation of functional nanoblocks using the AFM tip, activating molecules in the domain of the tip action. The compounds with reactive groups also open up ways to form soft matter with enhanced properties, for example, by copolymerization of two insoluble dyes to produce one phase solid with no aggregation during heating and so on. The production of dye solid films with required properties on nanostructured plastic substrates is one more challenge for future researches, which will be useful for organic electronic devices with a flexible plastic substrate.

Acknowledgements The paper is dedicated to the memory of Prof. Dr O.I. Tolmachev, who headed the dyes design and synthesis for more than 40 years. The authors express their thanks to Drs B. Grimm, D. Prescher, V. Kurdiukov and M. Kudinova for the dyes syntheses, Dr Yu. Kolomzarov, Mrs T. Doroshenko, Mr M. Seryk and Mr O. Navozenko for the films deposition. The authors are grateful to German Academic Exchange Service (DAAD) (Grant no. 91697212) for the purchase of the Polytec spectrometers, for funding of Dr K. Grytsenko's visits to Germany and to the Science and Technology Center (Grant nos. 2348, 3480, 4570, 5709) in Ukraine (www.stcu.int) for funding a significant part of this research.

References

1. K.P. Gritsenko, V.V. Petrov, D.A. Grinko, A.A. Kriuchin, Vacuum deposition of organic dyes and their optical properties, Abstr. Book:. 4 Sci. Conference Vacuum coatings-87, Riga, vol 2 (1987), p. 127
2. H. Böttcher, T. Fritz, J.D. Wright, Fabrication of evaporated dye films and their application. J. Mater. Chem. **3**, 1187 (1993)
3. K.P. Gritsenko, YuL Slominsky, K. Fedotov, Vacuum-deposited dye films and their optical properties. Proc. SPIE **3359**, 479 (1997)
4. S.R. Forrest, Ultrathin organic films grown by organic molecular beam deposition and related techniques. Chem. Rev. **973**, 1793 (1997)

5. R. Nitsche, Optical properties of organic semiconductors: from sub-monolayers to crystalline films, Diss. Dr. rer. nat., Dresden, p. 173 (2005)
6. S.A. Burke, J.M. Topple, P. Grutter, Molecular dewetting on insulators. J. Phys. Condensed Matter **21**, 1 (2009)
7. J.M. Topple, S.A. Burke, W. Li, S. Fostner, A. Tekiel, P. Grutter, Tailoring the morphology and dewetting of an organic thin film. J. Phys. Chem. C **115**, 217 (2011)
8. S. Bommel, Unravelling nanoscale molecular processes in organic thin films, Diss. Dr. rer. nat. Mathematisch-Naturwissenschaf. Fakultät der Humboldt-Universität zu Berlin, vol 158 (2015)
9. M. Beigmohamadi, Growth, structure and morphology of organic thin films, Ph.D. Technische Hochschule Aachen zur Erlangung, vol 147 (2007)
10. P. Frank, Thin film growth of rod-like and disc-shaped organic molecules on insulator and noble metal surfaces, PhD Thes., Graz University of Technology, vol 166 (2009)
11. P. Graziosi, Materials engineering in hybrid spintronic devices, Diss. Dr. rer. nat. Parma, vol 124 (2010)
12. K. Grytsenko, T. Doroshenko, Yu. Kolomzarov, O. Lytvyn, M. Serik, O. Tolmachev, Yu. Slominski, S. Schrader, Growth and optical properties of film of dyes and dye-in-polymer matrix, deposited by evaporation in vacuum. Semicond. Phys. Quantum Electron Optoelectron. **13.2**, 177 (2010)
13. A.L. Briseno, S.C.B. Mannsfeld, S.A. Jenekhe, Z. Bao, Y. Xia, Introducing organic nanowire transistors. Mater. Today **11.4**, 38 (2008)
14. K. Xiao, I.N. Ivanov, A.A. Puretzky, Z. Liu, D.B. Geohegan, Directed integration of tetracyanoquinodimethane-Cu organic nanowires into prefabricated device architectures. Adv. Mater. **18**, 2184 (2006)
15. Y.S. Zhao, P. Zhan, J. Kim, C. Sun, J. Huang, Patterned growth of vertically aligned organic nanowire waveguide arrays. ACS Nano **4.3**, 1630 (2010)
16. L. Tavares, J. Kjelstrup-Hansen, K. Thilsing-Hansen, H.-G. Rubahn, Organic nanofibers integrated by transfer technique in field-effect transistor devices. Nanoscale Res. Lett. **6**, 319 (2011)
17. K. Grytsenko, P. Lytvyn, T. Doroshenko, O. Navozenko, O. Fedoryak, O. Tolmachev, Yu. Slominskii, Yu. Briks, V. Ksianzou, S. Schrader, Evaporable self-assembled dyes with tuned optical properties for nanostructures, Abstr Book: 4th EOS Topical Meeting on Optical Microsystems, Capri, September 26–28, 38 (2011)
18. D. Frattarelli, M. Schiavo, A. Facchetti, M.A. Ratner, T.J. Marks, Self-assembly from the gas-phase: design and implementation of small-molecule chromophore precursors with large nonlinear optical responses. J. Am. Chem. Soc. **131.35**, 12595 (2009)
19. F. Holzmüller, N. Gräßler, M. Sedighi, E. Müller, M. Knupfer, O. Zeika, K. Vandewal, C. Koerner, K. Leo, H-aggregated small molecular nanowires as near infrared absorbers for organic solar cells. Org. Electron. **45**, 198 (2017)
20. G. Vyas, P. Dagar, S. Sahu, Exponential increase in the on–off ratio of conductance in organic memory devices by controlling the surface morphology of the devices. Appl. Phys. A **124**, 369 (2018)
21. T. Thiele, D. Prescher, R. Ruhmann, D. Wolf, Synthesis of 4-(1H,1H-perfluoroalkoxy)-4′-(6-methacryloyloxy-hexyloxy)-azobenzenes and their liquid crystalline intermediates. J. Fluorine Chem. **85**, 155 (1997)
22. S. Schrader, R. Wortmann, D. Prescher, K. Lukaszuk, A. Otto, Solvatochromy and electrooptical study of new fluorine-containing chromophores. Proc. SPIE **3474**, 14–22 (1998)
23. O.I. Tomachev, N.V. Pilipchuk, O.D. Kachkovsky, YuL Slominski, V.Ya. Gayvoronsky, E.V. Shepelyavyy, S.V. Yakunin, M.S. Borodyn, Spectral and non-linear optical properties of cyanine bases derivatives of benzo[c, d]indole. Dyes Pigm. **74**, 195 (2007)
24. W. Rettig, M.L. Dekhtyar, A.I. Tolmachev, V.V. Kurdyukov, Two heterocyclic merocyanine classes and their optical properties in relation to the donor-acceptor strength of end substituents. Chem. Het. Compounds **47.10**, 1244 (2012)
25. A.I. Tolmachev, Y.P. Pyryatinskii, V.V. Kurdyukov, A.D. Kachkovsky, Dimethine merocyanines derivatives of 2,6-di-*tert*-butylcyclohexa-2,5-dienone Absorption and low temperature fluorescence spectra. Ukrainian Chem. J. **804**, 117 (2014)
26. O. Dimitriev, K. Grytsenko, P. Lytvyn, T. Doroshenko, O. Tolmachev, Yu. Slominskii, Yu. Briks, S. Schrader, R.-D. Schulze, J. Friedrich, Substrate-induced self-assembly of donor-acceptor type compounds with terminal thiocarbonyl groups. Thin Solid Films **539**, 127 (2013)
27. K.P. Gritsenko, A.M. Krasovsky, Thin film deposition of polymers by vacuum degradation. Chem. Rev. **103.9**, 3607 (2003)
28. K. Grytsenko, T. Doroshenko, Yu. Kolomzarov, V. Prokopets, O. Fedoriak, R. Zelinski, O. Lytvyn, D. Prescher, B. Grimm, V. Ksianzou, S. Schrader, O. Tolmachev, Yu. Slominskii, V. Kurdiukov, G. Smirnova, Research on the growth of dye film in vacuum in situ. Proc. SPIE **6999**, 69991Z-69991Z-6 (2008)
29. M.M. Sieryk, T.P. Doroshenko, K.P. Grytsenko, O.M. Navozenko, O.I. Tolmachev, Y.L. Slominski, S. Schrader, The influence of temperature on optical properties of merocyanine dye thin films. Semicond. Phys. Quantum Electron. Optoelectron. **16.1**, 91 (2013)
30. M. Sieryk, O. Dimitriev, T. Doroshenko, K. Grytsenko, Yu. Slominsky, O. Kachkovsky, Aggregation of derivatives of benz[C,D] indole dyes: effect of the side group and ambient temperatures, IEEE XXXIV International Sci. Conf. Electronics and Nanotechnology (ELNANO), Kyiv, 226 (2014)
31. L. Daehne, J. Tao, G. Mao, Surface morphological study of J-aggregate thin films by atomic force microscopy. Langmuir **14**, 565 (1998)
32. A. Ojala, Merocyanine dyes as donor materials in vacuum-deposited organic solar cells: insights into structure-property-performance relationships, Dr. Nat. Julius-Maximilian-Universität Würzburg, p. 204 (2011)
33. M.M. Sieryk, O.P. Dimitriev, Tuned aggregation and film self-assembly of monomethin-cyanine dyes through variation of their monomer structure. Semicond. Phys. Quantum Electron. Optoelectron. (On-line) **22.1**, 53 (2019)
34. A.A. Esteban, Solar Cell and Transistor Devices, Dr. Nat. Julius-Maximilian-Universität Würzburg, p. 178 (2015)
35. A. Liess, Structure-Property Relationships of Merocyanine Dyes in the Solid State: Charge Transport and Exciton Coupling, Dr. Nat. Julius-Maximilian-Universität Würzburg, p. 173 (2017)
36. L. Sun, S. Berkebile, G. Weidlinger, M. Denk, R. Denk, M. Hohage, G. Koller, F.P. Netzer, M.G. Ramsey, P. Zeppenfeld, Layer resolved evolution of the optical properties of a-sexithiophene thin films. Phys. Chem. Chem. Phys. (2012). https://doi.org/10.1039/c2cp42270k
37. N. Kleppmann, S.H.L. Klapp, Non-equilibrium surface growth in a hybrid inorganic-organic system, arXiv:1511.00587v2 [cond-mat.soft] 4 September 2016 (2016)
38. K. Grytsenko, P. Lytvyn, O. Navozenko, Yu. Kolomzarov, J. Briks, V. Kurdukov, Yu. Slominskii, O. Tolmachev, V. Ksianzou, S. Schrader, Evaporable dyes with absorption in blue region, Abstr. Book: Conference Nanotechnology and nanomaterials, August 29–September 1, Bukovel, p. 183 (2013)
39. V.G. Kravets, G. Zoriniants, C.P. Burrows, F. Schedin, A.K. Geim, W.L. Barnes, A.N. Grigorenko, Composite Au nanostructures for fluorescence studies in visible light. Nano Lett. **10**, 874 (2010)
40. I.V. Barca, A.P. Brown, M.P. Andrews, T. Galstian, Linear and nonlinear optical response of dye anchored to gold nanoparticles. Canad. J. Chem. **80**, 1625 (2002)
41. K.P. Gritsenko, A. Capobianchi, A. Convertino, J. Friedrich, R.D. Schulze, V. Ksensov, S. Schrader, Polymer-metal composite thin

film prepared by co-evaporation in vacuum, in *Polymer surface modification and polymer coatings by dry process technologies*, ed. by S. Iwamori (Research Signpost, Kerala, 2005), pp. 85–109
42. G. Bauer, J. Hassmann, H. Walter, J. Haglmuller, C. Mayer, T. Schalkhammer, Resonant nanocluster technology—from optical coding and high quality security features to biochips. Nanotechnology **14**, 1 (2003)
43. K.G. Thomas, P. Kamat, Chromophore-functionalized gold nanoparticles. Acc. Chem. Res. **36**, 888 (2003)
44. H.-Y. Kim, D.H. Song, H. Yoon, J.S. Suh, Surface plasmon-enhanced dye-sensitized solar cells based on double-layered composite films consisting of TiO_2/Ag and TiO_2/Au nanoparticles. RSC Adv. **5**, 27464 (2015)
45. P. Podsiadlo, V.A. Sinani, J.H. Bahng, N.A. Kotov, Gold nanoparticles enhance the anti-leukemia action of a 6-mercaptopurine chemotherapeutic agent. Langmuir **24**, 568 (2008)
46. K.M. Mayer, F. Hao, S. Lee, P. Nordlander, J.H. Hafner, A single molecule immunoassay by localized surface plasmon resonance. Nanotechnol. **21**, 1 (2010)
47. K. Grytsenko, P. Lytvyn, O. Tolmachev, Y. Slominskii, Y. Briks, V. Ksianzou, S. Schrader, Sulphur-terminated dye film growth in vacuum and their self-assembled structures, 2-nd Ukrainian-French Seminar and 7-th Workshop. In: Functional nanomaterials and devices, Kyiv, p. 153 (2013)
48. K. Grytsenko, P. Lytvyn, T. Doroshenko, O. Tolmachev, Y. Slominskii, Y. Briks, V. Ksianzou, S. Schrader, T.Galstian, Kinetics of dye film growth in vacuum and their self-assembled structures, Abstr. Book: Winter school on organic electronics, Planneralm, p. 73 (2012)
49. K. Grytsenko, P. Lytvyn, T. Doroshenko, Yu. Kolomzarov, O. Tolmachev, Y. Slominskii, V. Ksianzou, S. Schrader, O. Sakhno, Dye deposit formation in vacuum on the gold nanocluster surface, Abstr. Book: Nanotechn. & nanomaterials, Bukovel, p. 182 (2013)
50. K. Grytsenko, P. Lytvyn, T. Doroshenko, Y. Kolomzarov, V. Kurdyukov, Y. Slominskii, O. Tolmachev, Morphology of sulphur-terminated compound deposits, condensed on different substrates in vacuum. Semicond. Phys. Quantum Electron. Optoelectron. **18.4**, 433 (2015)
51. K. Grytsenko, S. Schrader, H. Detert, Ultra-stable dye-filled polytetrafluoroethylene thin films. Nanosci. Technol. **12**, 1 (2014)
52. L. Ivanov, K. Grytsenko, Y. Kolomzarov, O. Tolmachev, Y. Slominskii, S. Schrader, Organised structures in PTFE film filled with dye and metal nanoparticles and novel research trends, In Book: Abstr. Conference Polycomtrib-2015, Gomel, p. 29 (2015)
53. K. Grytsenko, O. Tolmachev, Y. Slominski, Evaporable dyes with reactive group, Abstr. Book: EMRS Spring Meeting, Strasbourg, p. Q-6 (2008)
54. K. Grytsenko, O. Tolmachev, Y. Slominski, Evaporable dyes with reactive group, Abstr. book: conference ICEL-7, Dresden, p. 180 (2008)
55. E. Tolstopyatov, K. Grytsenko, Y. Kolomzarov, P. Lytvyn, O. Navozenko, S. Schrader, O. Tolmachev, Y. Slominsky, O. Sakhno, Polymeric dye by gas phase deposition, Abstr. Book: Internat. Conf. Polymer composites and tribology, Gomel, p. 131 (2013)
56. K. Gytsenko, Yu. Slominskii, Polymeric dye film deposition in vacuum. Nanosci. Technol. **4**(2), 1 (2017)
57. N. Kashiwazaki, Iodized polymeric Yb-diphthalocyanine films prepared by plasma polymerization method. Jpn. J. Appl. Phys. **31.16A**, 1892 (1992)
58. N. Inagaki, S. Tasaka, Y. Ikeda, Plasma polymerization of copper phthalocyanine and application of the plasma polymer films to NO_2 gas sensor device. J. Appl. Polym. Sci. **55.10**, 1451 (1995)
59. M. Inoue, H. Morita, Y. Takai, T. Mizutani, M. Ieda, Photovoltaic cells of merocyanine dye polymer thin films prepared by plasma polymerization method. Jpn J Appl Phys **27.6**, 1059 (1988)
60. F. Homilius, A. Heilmann, C. von Borzyskowski, Plasma polymer thin films with encapsulated dye molecules and silver nanoparticles. Surf. Coat. Technol. **75.1**, 594 (1995)
61. I. Blaszczyk-Lezak, F.J. Aparicio, A. Borras, A. Barranco, A. Alvarez-Herrero, M. Fernandez-Rodrıguez, A.R. Gonzalez-Elipe, Optically active luminescent perylene thin films deposited by plasma polymerization. J. Phys. Chem. C **113**, 431 (2009)
62. F.J. Aparicio, A. Borras, I. Blaszczyk-Lezak, A. A. Alvarez-Herrero, M. Fernandez-Rodrıguez, A.R. Gonzalez-Elipe, A. Barranco, Luminescent and Optical Properties of Nanocomposite Thin Films Deposited by Remote Plasma Polymerization of Rhodamine 6G, Plasma Process. Polym. 6 (WILEY-VCH Verlag GmbH & Co. Weinheim, 2009) pp. 17–26
63. K.P. Gritsenko, E.M. Tolstopyatov, L.M. Yagupolskii, Y.L. Yagupolskii, M.M. Kremlev, Y.L. Slominsky, V.V. Shilov, G.P. Kovernik, Polymerisation of complex organic molecules in plasma, Abstr. Book: Conf. Ionizing Radiation and Polymers-98, Weinbohla, Germany, p. 11 (1998)
64. K. Gritsenko, E. Tolstopyatov, L.M. Yagupolskii, Y.L. Yagupolskii, M.M. Kremlev, Y.L. Slominsky, V.V. Shilov, G.P. Kovernik, Plasma polymerisation of complex organic molecules, Proc. Conf. Polymer Composites-98, Gomel, Belarus, p. 299 (1998)
65. J.A. Lim, F. Liu, S. Ferdous, M. Muthukumar, A.L. Briseno, Polymer semiconductor crystals. Mater. Today **13**(5), 14 (2010)
66. H-G. Rubahn, H. Sitter, G. Horowitz, K. Al-Shamery, Editors, Organic nanostructures for next generation devices, Springer Series in materials science 101 © (Springer, Heidelberg 2008), pp. 1–358
67. H-G. Rubahn, H. Sitter, G. Horowitz, K. Al-Shamery, Editors, Interface controlled organic thin films, 227 p. ISSN 0930-8989 ISBN 978-3-540-95929-8. https://doi.org/10.1007/978-3-540-95930-4 © (Springer, Berlin, Heidelberg, 2009)
68. M. de OliveiraHansen, J. Kjelstrup-Hansen, H-G Rubahn Pinning of organic nanofiber surface growth. Nanoscale **2**, 134 (2010)
69. A. Winkler, On the nucleation and initial film growth of rod-like organic molecules. Surf. Sci. **652**, 367 (2016)